Receiver function imaging in the western Himalaya

Warren B. Caldwell[1], Simon L. Klemperer[1], Jesse F. Lawrence[1], Shyam S. Rai[2]

[1] Department of Geophysics, Stanford University, Stanford, CA 94305-2215, U.S.A., warrenc@stanford.edu
[2] National Geophysical Research Institute, Hyderabad, India 500 007

Method

The western Himalaya is sparsely studied and imaged compared to the central and eastern portions of the range. In this work, we contribute to the existing body of crustal images of the western Himalaya using an array located at 80°E (Figure 1). The array consists of ~20 stations with ~10 km spacing arranged linearly from SW to NE across the Himalayan thrust belt, from the Main Frontal Thrust (MFT) to the South Tibetan Detachment (STD). The array was active in 2005-2006, and was operated by India's National Geophysical Research Institute (Mahesh and others, 2010).

We generate crustal images using stacking of P-S receiver functions. We calculate receiver functions using an iterative time-domain method and depth-convert them by back propagation in an assumed velocity model, then bin and stack them to obtain two-dimensional images. This method, called common conversion point (CCP) stacking, stacks coherent energy from crustal conversions at the appropriate depths, while simultaneously canceling random noise. This generates a two-dimensional image of converting layers in the crust and mantle, such as abrupt changes in density or lithology caused by faults or other boundaries. Our model has a bin size of 1 km in depth and 10 km horizontally.

Receiver functions were picked using three different Gaussian windows (1, 2.5, 5) and manual time windowing. Spurious receiver functions were discarded by hand, in addition to automated discarding based on signal-to-noise ratio. Of the 23 stations, several had few or zero usable receiver functions. Of the remaining stations, the mean number of quality receiver functions per station was ~40.

The distribution of events is asymmetrical, with a strong concentration of events coming from the northeast (Japan). The remaining events were scattered mainly to the east and southeast, including events from Indonesia. Few events came from the west, and almost none from the south. To account for this azimuthal variability, we weight the receiver functions by backazimuth by binning in 10° increments and scaling the receiver functions in each bin by the number of receiver functions in that bin. Thus each 10° increment (assuming it contains events) has an equal contribution to the final image.

Results

Our results at present (Figure 2) show a Moho conversion at 40-50 km depth in the well-sampled region of our model. This depth is consistent with the Moho depth observed beneath the HiCLIMB array to the east (Nabelek and others, 2009). The Moho is typically the strongest and most continuous conversion in a receiver-function image, but in our image the Moho is not significantly stronger than other conversions, and exhibits some discontinuity. Mafic lower crust and eclogitization of lower-crustal material can be responsible for weak Moho conversions, due to the resulting lessening of the impedance contrast between crust and mantle. These phenomena have been speculated to occur in the subducted Indian lower crust (Nabelek and others, 2009, Schulte-Pelkum and others, 2005), but not in regions as close to the foreland as our study location.

For the HiCLIMB array (85°E, see Figure 1), Nabelek and others (2009) showed a strong azimuthal dependence in Moho visibility, with arrivals from the north illuminating the Himalayan Moho well, and arrivals from the south illuminating it poorly (the former being due to oblique incidence on a northward-dipping Moho and the latter being due to orthogonal incidence, which minimizes P to S conversions). The events recorded on our array were heavily-distributed in the northeast (approximately 5 times more northern events than southern events), so if the Moho in this region exhibits the same dip characteristics as in the nearby HiCLIMB region, our weak Moho is unlikely to be the result of weakly-illuminating southern events.

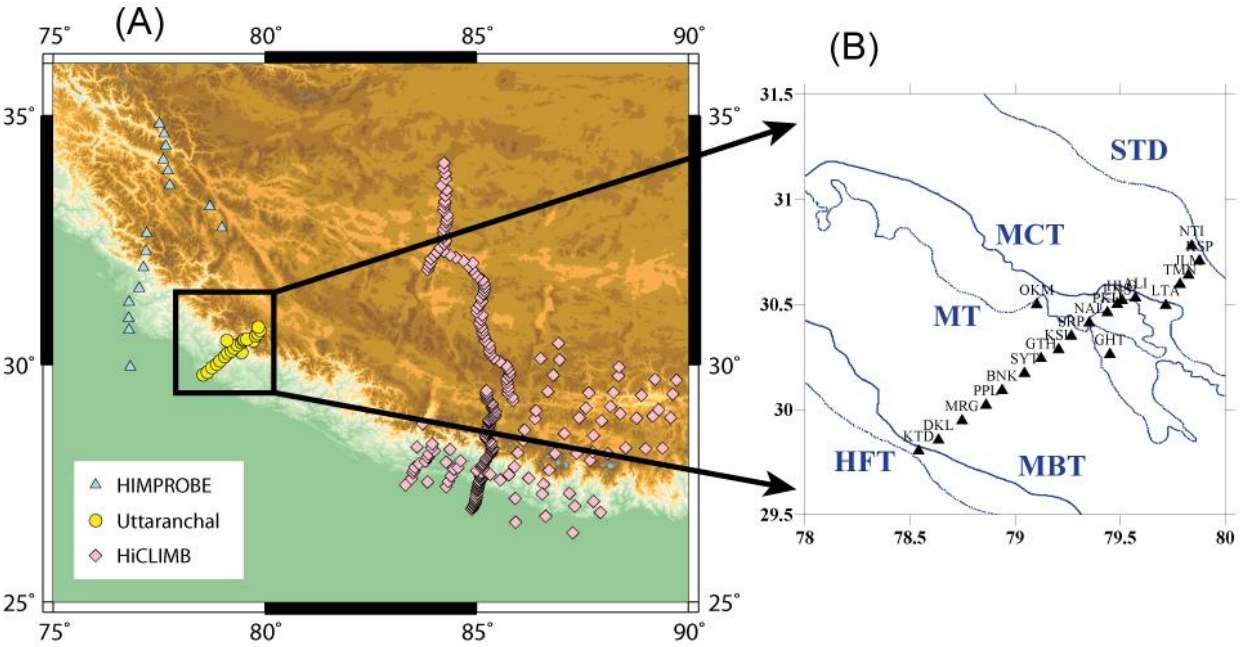

Figure 1. (A) Location of Uttaranchal broadband array used for this study in relation to nearby deployments. (B) Location of stations in relation to tectonic features. The array spans ~200 km and was composed of ~20 stations.

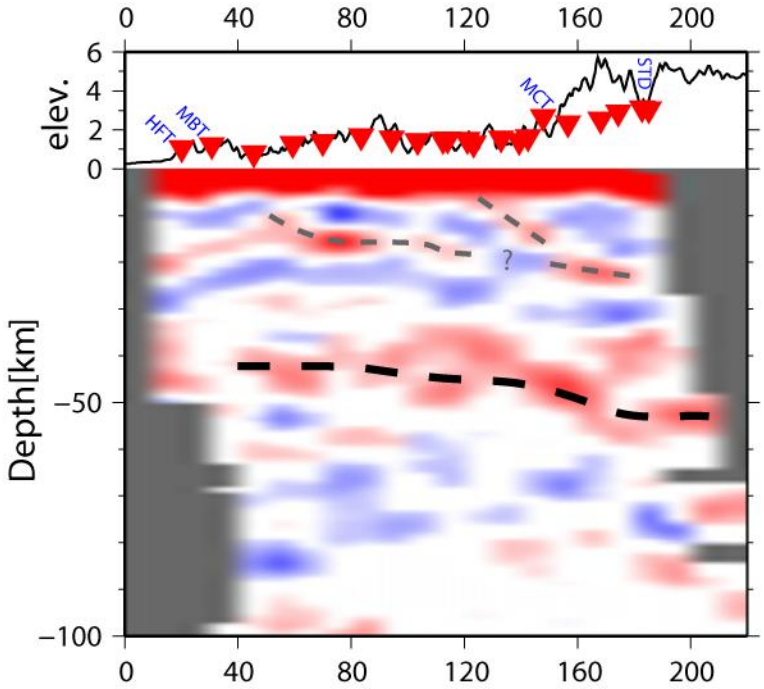

Figure 2. Receiver function CCP image with 10-km horizontal smoothing (red indicates positive impedance contrasts and blue indicates negative impedance contrasts). Bins with fewer than 25 rays are masked to gray. Upper panel shows vertically-exaggerated topography, station locations and approximate locations of the surface expressions of major faults. Approximate Moho shown with black dotted line. Thinner gray lines indicate impedance contrasts within the crust, likely thrust structures.

References

Mahesh, P., Rai, S.S., Sarma, P.R., Gupta, S., Sivaram, K., and Suryaprakasam, K., 2010, High resolution earthquake location and 3-D velocity imaging of crust beneath the Kumaon Himalaya, *in* Leech, M.L., and others, eds., Proceedings for the 25th Himalaya-Karakoram-Tibet Workshop: U.S. Geological Survey, Open-File Report 2010-1099, 2 p.

Nabelek, J., and others, 2009, Underplating in the Himalaya-Tibet Collision Zone Revealed by the Hi-CLIMB Experiment, Science, 325, 1371-1374.

Schulte-Pelkum, V., and others, 2005, Imaging the Indian subcontinent beneath the Himalaya, Nature, 435, 1222-1225.

Cite as: Caldwell, W.B, Klemperer, S.L., Lawrence, J.F. and Rai, S.S., 2010, Receiver function imaging in the western Himalaya, *in* Leech, M.L., and others, eds., Proceedings for the 25th Himalaya-Karakoram-Tibet Workshop: U.S. Geological Survey, Open-File Report 2010-1099, 2 p. [http://pubs.usgs.gov/of/2010/1099/caldwell/].